Ecotoxicology and Environmental Safety 242 (2022) 113888

Contents lists available at ScienceDirect

Ecotoxicology and Environmental Safety

journal homepage: www.elsevier.com/locate/ecoenv

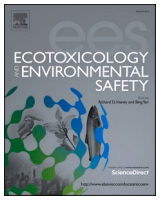

Systematic impacts of fluoride exposure on the metabolomics of rats

Shiyuan Zhao [a,1], Jinxiu Guo [a,1], Hongjia Xue [b], Junjun Meng [a], Dadi Xie [c], Xi Liu [d], Qingqing Yu [e,f], Haitao Zhong [a,*], Pei Jiang [a,*]

[a] Translational pharmaceutical laboratory of Jining First People's Hospital, Jining Medical University, Jining 272000, China
[b] Faculty of Science and Engineering, University of Nottingham Ningbo China, Ningbo 315100, China
[c] Department of Endocrinology, Tengzhou Central People's Hospital, Tengzhou 277500, China
[d] Department of Pharmacy, Linfen People's Hospital, Linfen 041000, China
[e] Department of Oncology, Jining First People's Hospital, Jining Medical University, Jining 272000, China
[f] Laboratory of Biochemistry and Biomedical Materials, College of Marine Life Science, Ocean University of China, Qingdao 266003, China

ARTICLE INFO

Edited by: Dr. Caterina Faggio

Keywords:
Fluoride
Fluorosis
Gas chromatography-mass spectrometry
Toxicity mechanism
Metabolomics
Biomarker

ABSTRACT

Fluoride is widely present in the environment. Excessive fluoride exposure leads to fluorosis, which has become a global public health problem and will cause damage to various organs and tissues. Only a few studies focus on serum metabolomics, and there is still a lack of systematic metabolomics associated with fluorosis within the main organs. Therefore, in the current study, a non-targeted metabolomics method using gas chromatography-mass spectrometry (GC-MS) was used to research the effects of fluoride exposure on metabolites in different organs, to uncover potential biomarkers and study whether the affected metabolic pathways are related to the mechanism of fluorosis. Male Sprague-Dawley rats were randomly divided into two groups: a control group and a fluoride exposure group. GC-MS technology was used to identify metabolites. Multivariate statistical analysis identified 16, 24, 20, 20, 24, 13, 7, and 13 differential metabolites in the serum, liver, kidney, heart, hippocampus, cortex, kidney fat, and brown fat, respectively, in the two groups of rats. Fifteen metabolic pathways were affected, involving toxic mechanisms such as oxidative stress, mitochondrial damage, inflammation, and fatty acid, amino acid and energy metabolism disorders. This study provides a new perspective on the understanding of the mechanism of toxicity associated with sodium fluoride, contributing to the prevention and treatment of fluorosis.

1. Introduction

Fluorides are naturally widespread in the environment, in water, soil, and plants (Jha et al., 2011; Singh et al., 2018). The main sources of human fluoride exposure are drinking water, dental products and food (Guissouma et al., 2017; Srivastava and Flora, 2020). Low-dose fluoride exposure can prevent dental caries (Whelton et al., 2019), but high-dose fluoride exposure and long-term accumulation may lead to fluorosis (Wei et al., 2019). The limit of fluorine in drinking water is 1.5 mg/L, according to the World Health Organization (Patil et al., 2018). Nevertheless, the risk of chronic endemic fluorosis still exists in many countries and regions on earth (McGill, 1995; Saeed et al., 2020; Yuan et al., 2020). In addition to skeletal fluorosis (Sellami et al., 2020) and dental fluorosis (Moimaz et al., 2015), excessive fluoride accumulation in the body also causes damage to other organs and tissues such as the brain (Agalakova and Nadei, 2020), liver (Malin et al., 2019), kidney (Dharmaratne, 2019), heart (Quadri et al., 2018), thyroid (Kheradpisheh et al., 2018), testes (Kumar et al., 2020), and spinal cord (Qing-Feng et al., 2019).

Fluoride is mainly absorbed in the stomach and intestines (Buzalaf and Whitford, 2011). Studies have shown that fluoride can penetrate the blood-brain barrier, cause brain metabolic disorders, inhibit related neural enzymes, and affect the morphology of brain synapses (Niu et al., 2018). Fluoride can also affect the density, morphology and motility of rat sperm (Gupta et al., 2007). Previous studies have shown that fluoride may poison the immune system, reduce the number of macrophages (De la Fuente et al., 2016), increase lipid peroxidation and increase pro-inflammatory cytokines. Acute fluoride exposure may also lead to

* Correspondence to: Jining First People's Hospital, Jining Medical University, Jiankang Road, Jining 272000, China.
E-mail addresses: zhaoshiyuan94@163.com (S. Zhao), guojx1116@163.com (J. Guo), hongjiaxue@126.com (H. Xue), M16619867832@163.com (J. Meng), xdd_wdyx@sina.com (D. Xie), liuxi418@163.com (X. Liu), yuqingqing_lucky@163.com (Q. Yu), haitao_zhong@163.com (H. Zhong), jiangpeicsu@sina.com (P. Jiang).
[1] These authors contributed equally to this work.

https://doi.org/10.1016/j.ecoenv.2022.113888
Received 24 March 2022; Received in revised form 9 July 2022; Accepted 14 July 2022
Available online 21 July 2022

myocardial injury and induce myocarditis (Panneerselvam et al., 2019).

Fluoride has a systemic effect on the body, involving a variety of organs and tissues, but there is still a lack of systematic and comprehensive studies on the observation of metabolite changes from the perspective of metabolomics. Metabolomics are not only sensitive to organ-specific toxicity but also provide information about the mechanisms involved in organs and tissues (Johnson et al., 2016). To the best of our knowledge, only two studies have investigated serum metabolites of fluoride exposure in rats (Li et al., 2021; Yue et al., 2020), and there is no metabolomic analysis of the main target organs of fluoride exposure. The metabolomics study of eight organs and tissues in this study will further explore the toxic mechanism of fluoride exposure and its impact on metabolic levels, and provide new biological insights to promote the diagnosis and treatment of fluorosis.

We carried out a metabolomics study on male Sprague-Dawley rats exposed to sodium fluoride, using gas chromatography-mass spectrometry (GC-MS). Changes in metabolite levels compared to the control group were detected and confirmed by multivariate statistical analysis, to investigate the relationship between differential metabolites and metabolic pathways and mechanisms of fluorosis.

2. Material and methods

2.1. Chemicals and reagents

Sodium fluoride (purity ≥ 99.99 %, metals basis) was purchased from Aladdin Reagent Co., Ltd. (Shanghai, China). Heptadecanoic acid (purity ≥ 98 %) was purchased from Sigma-Aldrich Chemical Co., Ltd. (MO, USA) as an internal standard compound in gas chromatography-mass spectrometry analysis. Pyridine and methanol were obtained from Sinopharm Chemical Reagent Co., Ltd. (Shanghai, China). O-methylhydroxylamine hydrochloride (purity ≥ 98 %) was purchased from J&K Scientific Co., Ltd. (Beijing, China). N,O-Bis(trimethylsilyl) trifluoroacetamide with trimethylchlorosilane (BSTFA + 1 % TMCS) (v/v) was purchased from Aladdin Reagent Co., Ltd. (Shanghai, China), and the water was supplied from Hangzhou Wahaha Company (Hangzhou, China).

2.2. Animals and treatment

Eight-week-old male Sprague Dawley rats were acquired from Jining Medical University. After acclimatization to a standard diet for 1 week, 12 rats were randomly designated to the control group (n = 6) and fluoride exposure group (n = 6). The exposure dose and length were determined according to our research and reported literature (Jiang et al., 2019; Faibish et al., 2016; Suzuki et al., 2015; Suzuki and Bartlett, 2014; Yue et al., 2020). The fluoride exposure group was provided with water containing the sodium fluoride that is present in drinking water (a concentration of 100 mg/L), for 6 weeks; the control group was provided with water. After 6 weeks, blood was extracted from the rats and then they were deeply anesthetized with isoflurane. Next, the rats were dissected on the ice, and the tissues (liver, kidney, heart, hippocampus, cortex, kidney fat, and brown fat) were quickly and carefully removed. The tissue samples were washed with phosphate-buffer (pH 7.2), immediately frozen in liquid nitrogen, and stored in a refrigerator at − 80 °C for later use. All experimental procedures were performed in accordance with the Regulations of Experimental Animal Administration issued by the State Committee of Science and Technology of the People's Republic of China, and approved by the University Ethics Committee (No. JNRM-2021-DW-052).

2.3. Sample preparation

Serum samples: The collected blood was immediately centrifuged at 5000 rpm for 5 min to obtain serum, then 100 μL serum was mixed with 350 μL methanol (containing 100 μg/mL heptadecanoic acid as an internal standard). The mixture was vortexed and centrifuged at 14,000 rpm for 15 min at 4 °C. Supernatant was taken and dried with nitrogen at room temperature. Next, 80 μL of pyridine solution containing 15 mg/mL of o-methylhydroxylamine hydrochloride was added and well mixed, and then heated in a water bath at 70 °C for 90 min. The sample was mixed with 100 μL of BSTFA + 1 % TMCS and incubated at 70 °C for 60 min to obtain a derivatization solution. After centrifugation and filtration through a 0.22-μm millipore filter, the solution was used for GC-MS analysis.

Tissue samples: 50-mg tissue samples were homogenized by adding 1 mL methanol. The tissue homogenate was added with 1 mg/mL internal standard, and then centrifuged at 14,000 rpm for 15 min at 4 °C to obtain the supernatant. Information about the remaining preparation steps are provided in the description of preparation of the serum samples.

Quality control sample (QCs): The pooled QC samples were prepared by combining the small aliquots of the control group and the fluoride exposure group.

2.4. GC-MS analysis

Analysis was performed with a 7890B-7000C GC-MS (Agilent Technologies, CA, USA). The specific operation conditions of chromatography were as follows: the chromatographic analysis was carried out with a HP-5MS capillary column, and the carrier gas was high purity helium flowing at 1 mL/min. The temperature of injection was 280 °C, and the injection volume was 1 μL with the split mode (50:1). Using a programmed heating method, the initial temperature was 60 °C for 4 min, which then increased to 300 °C at 8 °C/min, and was then maintained for 5 min. The conditions for mass spectrometry analysis were as follows: The ionization method used electrospray ionization, the ion source temperature was 230 °C, and the transfer line temperature was 250 °C. The ionization voltage was 70 EV and full scan mode was adopted with a quality scanning range of m/z 50–800. QC samples were inserted as every sixth sample to evaluate the stability of the instrument and the reproducibility of the entire process of analysis.

2.5. Multivariate statistical analyses and data processing

The primary GC-MS data were processed by Agilent Unknowns analysis software and Masshunter quantitative analysis software (Agilent Technologies, CA, USA). These data included peak extraction, removal of peaks with a signal-to-noise ratio less than three, and peak deconvolution (Dunn et al., 2012). The metabolites were identified by comparing the secondary mass spectrum of the compound with the NIST 14.0 database. The content ratio of various metabolites was quantified by the peak area normalization method, which is the ratio of each peak area to the total peak area. SIMCA-P 14.0 software (Umetrics,Umea, Sweden) was used to perform principal component analysis (PCA), partial least squares-discriminant analysis (PLS-DA), and orthogonal partial least squares-discriminant analysis (OPLS-DA) of the control group and the fluoride exposure group to determine whether there is a significant difference between them. At the same time, two-tailed student's t-tests were performed using SPSS 19.0 (SPSS Inc, Chicago, IL, USA) to further test the difference between the two groups. Metabolites with variable importance in projection (VIP) values > 1.0 in the OPLS-DA analysis and p values < 0.05 in the two-tailed student's t-tests were considered as potential discriminant metabolites. The finalized set of discriminant metabolites were imported into MataboAnalyst 5.0 (http://www.metaboanalyst.ca) and the Kyoto Encyclopedia of Genes and Genomes (KEGG; http://www.kegg.jp) for metabolic pathway analysis to understand the mechanisms of change in metabolic pathways. Pathways with impact values > 0 and P values < 0.05 were considered to be significantly affected metabolic pathways.

3. Results

3.1. Clinical parameters

The rats in both the fluoride exposure group and the control group survived to the end of the experimental periods and without becoming moribund. There was no significant difference in initial body weight between groups, with a trend to lower final body weights in rats after six weeks of fluoride exposure (Fig. 1A). The statistical changes in the water intake and organ weight of the rats over six weeks are summarized (Fig. 1B and Fig. 1C), which indicates that there was no significant differences between the fluoride exposure group and the control group. Fig. 1D showed the representative H&E-stained images of organs for rats. The control group showed no significant signs of edema, inflammatory cell infiltration, or necrosis in the liver, kidney, heart and brain tissues. However, pathological images of the fluoride exposure group showed diffuse hydropic degeneration, swollen cells, sparse cytoplasm (shown by black arrows), and irregular arrangement of hepatocyte cords in the liver tissue. In the kidney tissue, the epithelial cells of renal tubules showed hydropic degeneration. The cytoplasm was sparse (shown by black arrows). And the tubular structure was unclear. Cardiac tissue occasionally exhibited myocardial cell necrosis and calcification (shown by black arrows), and no obvious gliosis in the hippocampus.

3.2. GC-MS total ion chromatograms of serum and tissue samples

The total ion chromatograms of QCs are shown in Fig. 1E. All samples had a strong signal response, and a variety of metabolites were detected with large peak capacity within the running time. The retention time was stable and the chromatogram of each organ had good reproducibility.

3.3. Multivariate statistical analysis

OPLS-DA was established to analyze the data differences between the two groups. It can be seen from the score chart that the control group and the fluorine exposure group are clearly separated, indicating significant differences. Moreover, the differences within each group were small. The model parameters of each organ (Table S1) were all greater than 0.5 and close to 1, indicating that the fitting accuracy of the model was good. The reliability of the model was further verified by permutation tests. Fig. 2 shows that the intercept of the Q2 regression line on the y axis was less than 0, and all the Q2 values on the left were lower than the original points on the right.

Cluster analysis of the metabolite levels showed that although there was a slight overlap, most of the samples of the control group and the fluoride-exposed group were clustered into their two groups. The difference in metabolite levels between the two groups was large, and the difference between samples within each group was small (see Fig. 3).

3.4. Discriminant metabolites

The metabolites of the control group and of the fluoride exposure group were analyzed by SIMCA software and SPSS software (VIP>1, $P < 0.05$). There were 68 metabolites in the two groups showing significant differences. As the final metabolic site of all organs, serum is of great significance for finding biomarkers of fluoride exposure or fluorosis. The levels of 16 metabolites in the serum of the two groups were different, and most of these differences involved amino acids and organic acids. Fluoride exposure had a greater impact on the levels of metabolites in major organs such as the liver, kidney, heart, and brain. Specific information about metabolite changes is provided in Table 1.

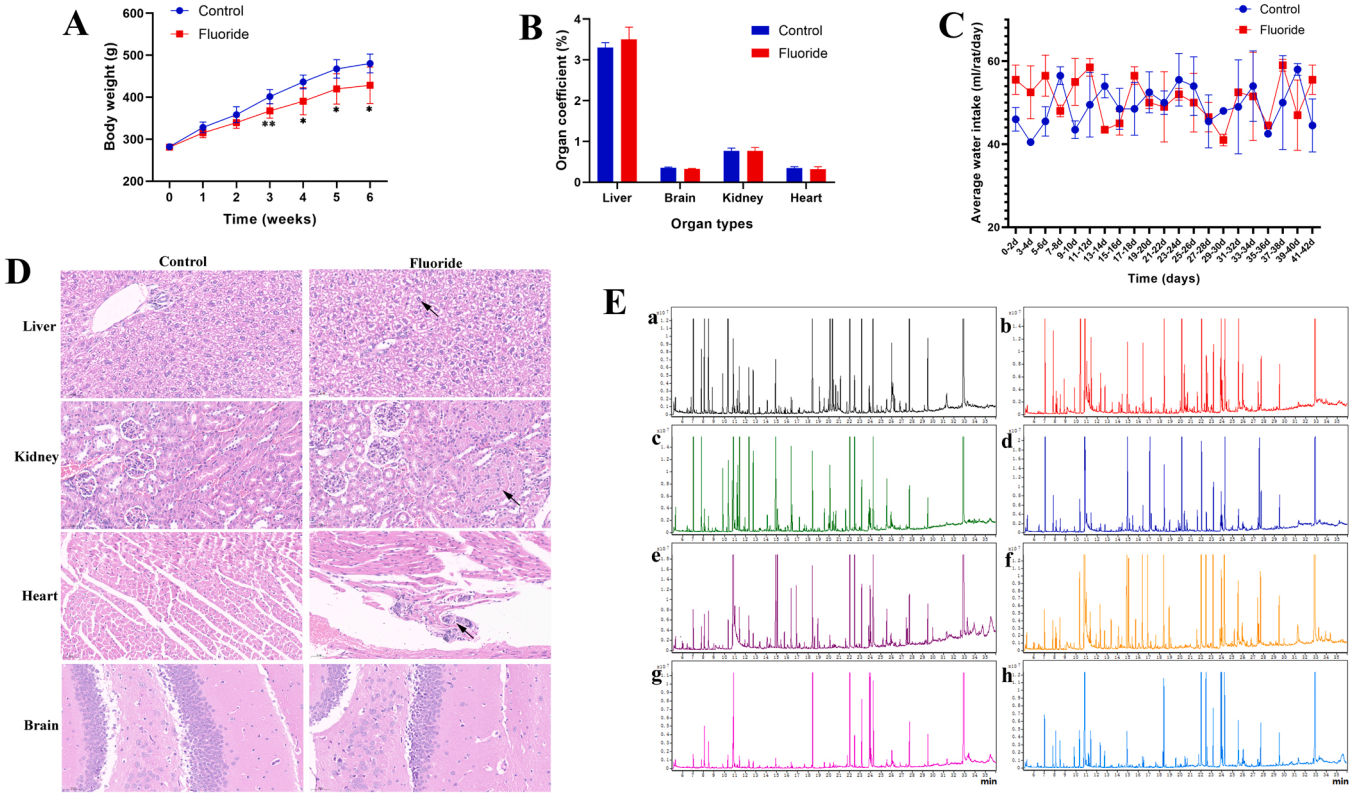

Fig. 1. Effect of fluoride on (A) body weight, (B) organ coefficient, (C) daily water intake, (D) pathological examination, (E) TIC images of QCs: (a) serum, (b) liver, (c) kidney, (d) heart, (e) hippocampus, (f) cortex, (g) kidney fat, and (h) brown fat. Values displayed are the mean ± SD, *p < 0.05 and **p < 0.01 indicate differences among the different groups.

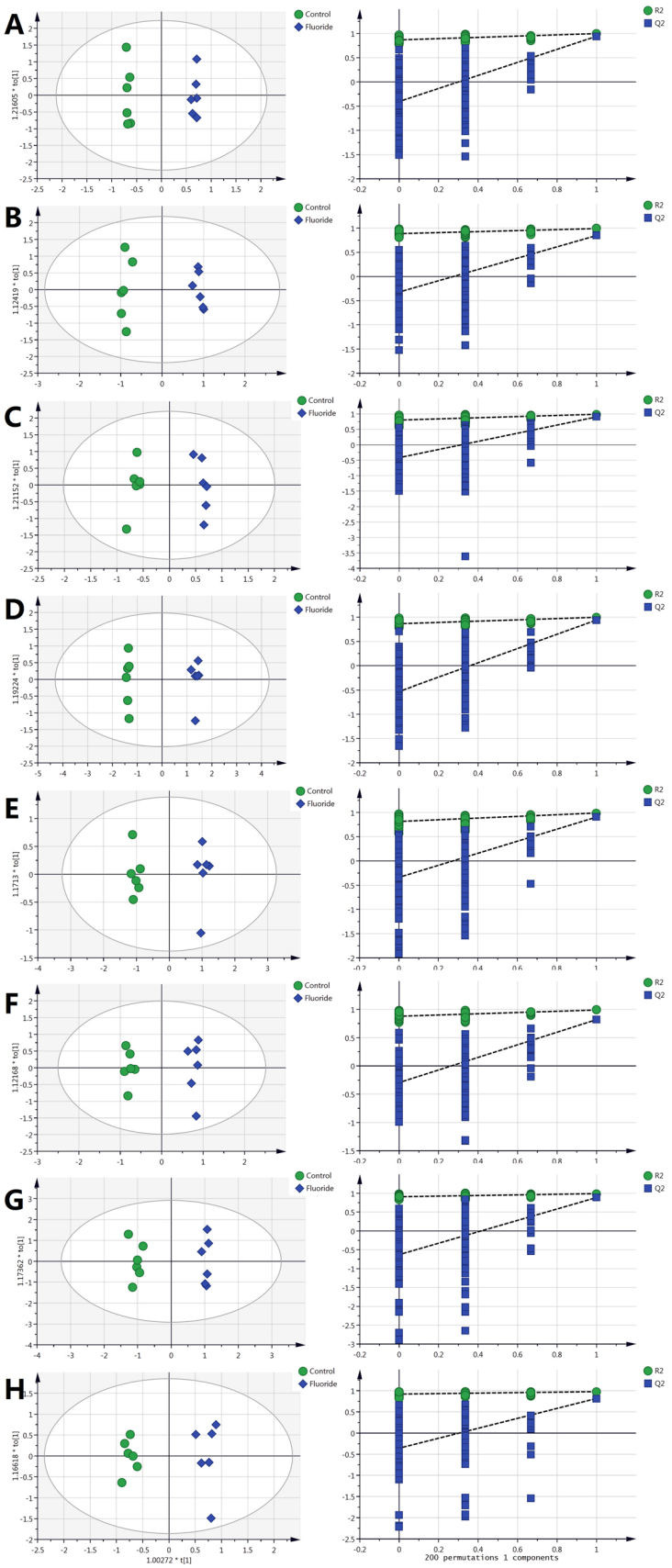

Fig. 2. OPLS-DA score chart and 200 permutation tests chart: (A) serum, (B) liver, (C) kidney, (D) heart, (E) hippocampus, (F) cortex, (G) kidney fat, and (H) brown fat.

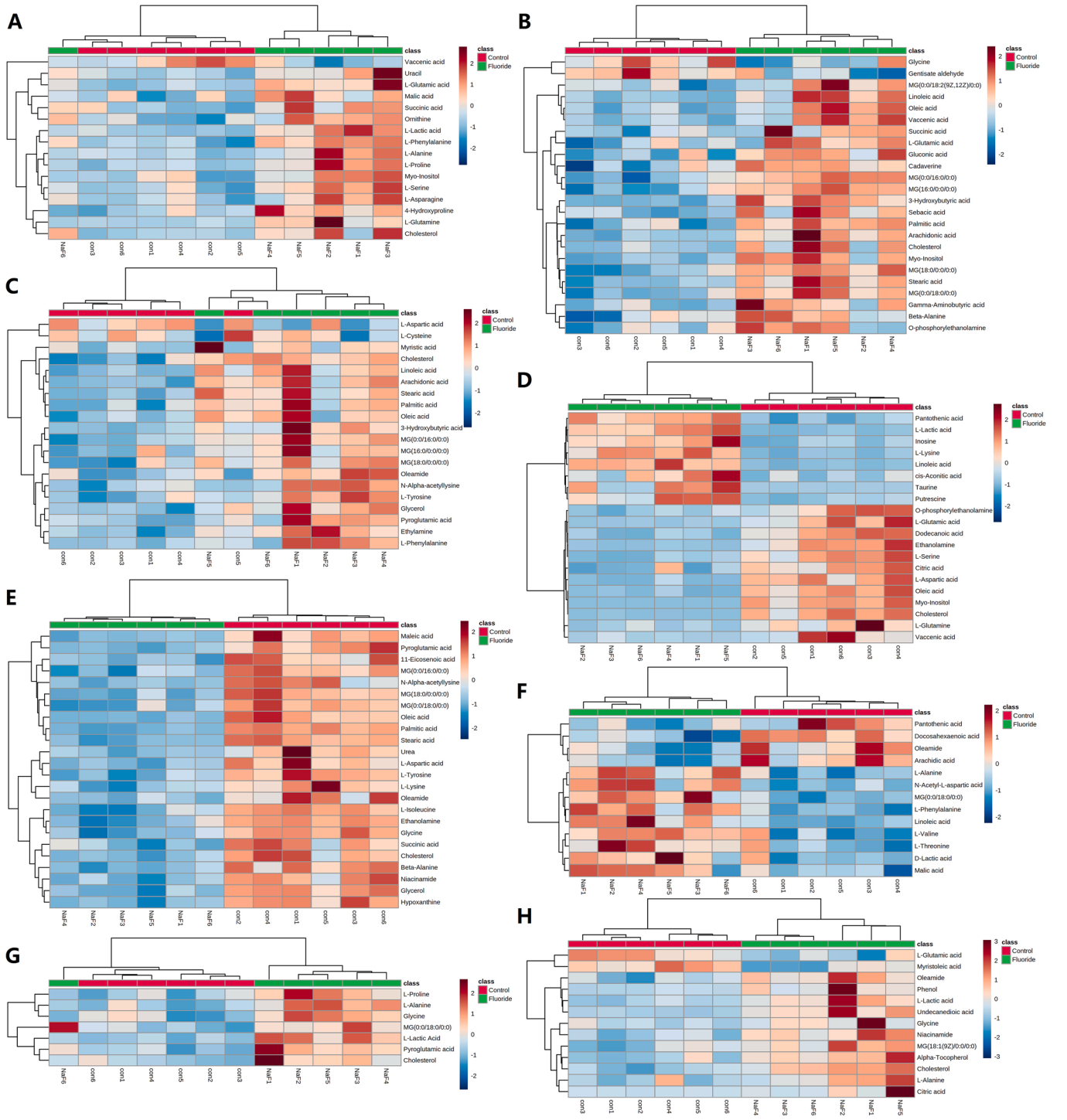

Fig. 3. Cluster analysis and heatmap of differential metabolites in the (A) serum, (B) liver, (C) kidney, (D) heart, (E) hippocampus, (F) cortex, (G) kidney fat, and (H) brown fat samples in the fluoride-exposed group compared to the control. The color indicates the significance of the different metabolites (blue, down-regulated; red, up-regulated). The rows represent samples and the columns represent metabolites.

3.5. Metabolic pathway analysis

The expression of 15 metabolic pathways were significantly different between the control group and fluoride exposure group (raw $P < 0.05$, impact > 0.05). The details of metabolic pathway analysis are presented in Table 2 and Fig. 4.

4. Discussion

Excessive fluoride exposure in the environment or drinking water can lead to chronic fluorosis (DenBesten and Li, 2011; Yuan et al., 2020). This can cause nervous system toxicity, and the heart, liver and kidneys are the most susceptive soft tissues to fluorosis. However, there are few studies on organ fluoride toxicity at the metabolic level. GC-MS has high detection sensitivity and can identify a large number of metabolites in the body (Papadimitropoulos et al., 2018). Through multivariate

Table 1
List of metabolites with changes in serum, liver, kidney, heart, hippocampus, cortex, kidney fat, and brown fat following fluoride exposure.

Metabolite	HMDB	Serum		Liver		Kidney		Heart		Hippocampus		Cortex		Kidney fat		Brown fat	
		VIP	FC	VIP	FC	VIP	FC	VIP	FC	VIP	FC	VIP	FC	VIP	FC	VIP	FC
3-Hydroxybutyric acid	HMDB0000357			2.134	3.230	2.153	2.557										
4-Hydroxyproline	HMDB0000725	1.065	1.454														
11-Eicosenoic acid	HMDB0034296									1.374	0.391						
Alpha-tocopherol	HMDB0001893															1.240	1.418
Arachidonic acid	HMDB0001043			1.756	1.469	1.386	1.614					1.832	0.407				
Beta-alanine	HMDB0000056			1.354	1.822					1.532	0.311						
Cadaverine	HMDB0002322			1.328	1.633												
Cholesterol	HMDB0000067	1.421	1.788	1.402	1.085	1.006	1.380	1.528	0.093	1.140	0.560			1.666	1.575	1.731	1.880
Cis-aconitic acid	HMDB0000072							1.003	2.597								
Citric acid	HMDB0000094							1.141	0.268							2.210	11.311
D-lactic acid	HMDB0001311											1.321	1.711				
Docosahexaenoic acid	HMDB0002183											1.196	0.723				
Dodecanoic acid	HMDB0000638							1.458	0.133								
Ethanolamine	HMDB0000149							1.426	0.995	1.226	0.795						
Ethylamine	HMDB0013231					1.214	1.302										
Gamma-aminobutanoic acid	HMDB0000112			1.573	2.201												
Gentisate aldehyde	HMDB0004062			1.224	0.603												
Gluconic acid	HMDB0000625			1.260	1.544												
Glycerol	HMDB0000131					1.480	1.608			1.206	0.537						
Glycine	HMDB0000123			1.033	0.650					1.189	0.544			2.020	1.468	1.618	2.844
Hypoxanthine	HMDB0000157									1.102	0.587						
Inosine	HMDB0000195							1.157	3.326								
L-alanine	HMDB0000161	1.563	1.986									1.439	1.631	2.371	1.904	1.064	1.416
L-aspartic acid	HMDB0000191	1.578	1.955			2.106	0.367	1.423	0.145	1.206	0.491						
L-cysteine	HMDB0000574					1.251	0.631										
L-glutamic acid	HMDB0000148	1.432	1.752	1.393	1.885			1.326	0.193							1.213	0.650
L-glutamine	HMDB0000641	2.159	5.811					1.325	0.194								
Linoleic acid	HMDB0000673			1.578	1.955	1.523	1.539	1.441	7.024			1.742	2.087				
L-isoleucine	HMDB0000172									1.001	0.662						
L-lactic acid	HMDB0000190	1.633	2.214					1.512	10.107					3.313	1.995	1.938	2.860
L-lysine	HMDB0000182							1.283	3.729	1.089	0.555						
L-phenylalanine	HMDB0000159	1.349	1.545			1.793	1.852					1.326	1.470				
L-proline	HMDB0000162	1.751	2.370											1.605	1.645		
L-serine	HMDB0000187	1.328	1.546					1.169	0.331								
L-threonine	HMDB0000167											1.259	1.308				
L-tyrosine	HMDB0000158					1.543	1.539			1.110	0.582						
L-valine	HMDB0000883											1.091	1.338				
Maleic acid	HMDB0000176									1.277	0.479						
Malic acid	HMDB0000156	1.071	1.380									1.361	1.695				
MG(0:0/16:0/0:0)	HMDB0011533			1.357	1.142	1.188	1.425			1.047	0.621						
MG(16:0/0:0/0:0)	HMDB0011564			1.474	1.287	1.062	1.345										
MG(0:0/18:0/0:0)	HMDB0011535			1.615	1.432					1.113	0.574	1.233	1.428	2.341	1.404		
MG(18:0/0:0/0:0)	HMDB0011131			1.391	1.209	1.008	1.297			1.018	0.636						
MG(0:0/18:2(9Z,12Z)/0:0)	HMDB0011538			1.940	1.375												
MG(18:1(9Z)/0:0/0:0)	HMDB0011567															1.141	1.551
Myo-inositol	HMDB0000211	1.070	1.358	1.115	1.351			1.610	0.045								
Myristic acid	HMDB0000806					1.053	1.290										
Myristoleic acid	HMDB0002000															1.763	0.380
N-acetyl-L-aspartic acid	HMDB0000812											2.247	3.855				
N-alpha-acetyllysine	HMDB0000446					1.510	1.552			1.318	0.432						
Niacinamide	NMDB0001406									1.020	0.616					1.387	1.601
Oleamide	HMDB0002117					1.328	1.549			1.615	0.221	1.842	0.382			1.517	1.832

(*continued on next page*)

Table 1 (*continued*)

Metabolite	HMDB	Serum		Liver		Kidney		Heart		Hippocampus		Cortex		Kidney fat		Brown fat	
		VIP	FC	VIP	FC	VIP	FC	VIP	FC	VIP	FC	VIP	FC	VIP	FC	VIP	FC
Oleic acid	HMDB0000207			1.788	1.426	1.010	1.312	1.317	0.241	1.342	0.454						
O-phosphoethanolamine	HMDB0000224			1.238	1.672			1.115	0.305								
Ornithine	HMDB0000214	1.082	1.589														
Palmitic acid	HMDB0000220			1.053	1.329	1.129	1.320			1.211	0.548						
Pantothenic acid	HMDB0000210							1.193	3.279			1.004	0.739				
Phenol	HMDB0000228															2.238	8.483
Putrescine	HMDB0001414							1.116	3.117								
Pyroglutamic acid	HMDB0000276					1.694	2.040			1.198	0.523			2.397	1.903		
Sebacic acid	HMDB0000792			1.853	2.739												
Stearic acid	HMDB0000827			1.532	1.336	1.216	1.459			1.268	0.509						
Succinic acid	HMDB0000254	1.533	2.091	1.410	2.070					1.452	0.326						
Taurine	HMDB0000251							1.492	7.478								
Vaccenic acid	HMDB0003231	1.182	0.658	1.707	1.361			1.098	0.277								
Undecanedioic acid	HMDB0000888															2.114	3.308
Uracil	HMDB0000300	1.847	3.017														
Urea	HMDB0000294									1.166	0.512						

VIP, variable importance in projection; FC, fold change = fluoride/control.

statistical analysis, 68 differential metabolites were found in the control group and the fluoride exposure group, and 15 metabolic pathways were affected. The interaction between pathways can be seen in Fig. 5. Herein, we discussed the metabolic effects of fluoride exposure in the whole body and major organs, respectively, and looked for potential biomarkers and the mechanism of organ damage, to explore the mechanism of toxicity and the methods of treatment intervention for fluorosis.

4.1. Serum metabolism analysis

The serum metabolome represents the final output of all organs and is a detailed systematic characterization of physiological state. The study of biomarkers in serum is helpful for the diagnosis of fluoride exposure and the changes in physiological state. A total of 16 differential metabolites, which may be used as potential biomarkers, were screened out through multivariate statistical analysis. The related metabolic pathways include arginine synthesis and proline metabolism, and glutathione metabolism, involving amino acid metabolism disorders, and urea cycle and energy metabolism disorders. The eight differential metabolites were amino acids, including L-alanine, L-proline, L-serine, L-glutamic acid, L-phenylalanine, L-asparagine, L-glutamine, and ornithine.

The levels of L-proline and 4-hydroxyproline in the serum of rats exposed to fluoride were both elevated. Proline can be synthesized from arginine and glutamic acid, and is the main amino acid constituting collagen, which helps maintain the strength and normal structure of connective tissues (including bones, cartilage, and the cardiovascular system) (Karna et al., 2020; Li and Wu, 2018; Wu et al., 2011). Abnormal metabolism of proline may affect the synthesis of collagen and further affect the structure of bone tissue. It is speculated that this may also be one of the causes of skeletal fluorosis. It has been proposed that proline may act as a neurotoxin and a metabotoxin, causing damage to nerve cells and nerve tissues (Nadler et al., 1988). The increase in mild or high levels of proline may be related to cancer and mental illness (Fonteh et al., 2007; Phang, 2019). Hydroxyproline is formed by hydroxylation of proline on a peptide chain under the action of proline hydroxylase. At the same time, collagen can be decomposed under the action of collagenase, hydroxyproline is then released, and in turn hydroxyproline in the blood increases (Wu et al., 2019). Hydroxyproline content can be used to characterize the content of collagen in tissue or biological samples (Li and Wu, 2018). The increase of hydroxyproline content in serum may be due to the increase of collagen catabolism, bone absorption, and bone tissue degradation, which is related to bone injury caused by fluorine. Hydroxyproline is related to Paget's disease (Zanglis et al., 2005), Alzheimer's disease (Chatterjee et al., 2021), and hydroxyprolinemia (Staufner et al., 2016). The levels of L-proline and 4-hydroxyproline can be used as potential biomarkers of fluoride exposure.

Ornithine, the core part of the urea cycle, plays an important role in the excretion of ammonia nitrogen in the body. Ornithine is the precursor for the synthesis of citrulline and arginine. The increased accumulation of ornithine in the blood of fluoride-exposed rats may be due to the decreased transport of ornithine to mitochondria, resulting in the reduction of ammonia load capacity. High concentrations of ammonia may have toxic effects on cells. High concentrations of ornithine have also been confirmed to be related to diseases such as hyperammonemia (Salvi et al., 2001), cancer (Ni et al., 2014), and gyrate atrophy of the choroid and retina (Simell and Takki, 1973). The high concentration of ornithine detected in our study was also similar to the results of Yue's study (Yue et al., 2020). The possibility of ornithine as a potential biomarker of fluoride exposure was demonstrated.

4.2. Liver metabolism analysis

The damage mechanism of fluoride exposure is different for different

Table 2
Metabolic pathways related to the fluoride exposure intervention mechanism.

Pathway name	Tissue	Match status	Hit	Raw p	FDR	Impact
Alanine, aspartate and glutamate metabolism	Serum	5/28	L-asparagine, L-alanine, L-glutamic acid, L-glutamine, Succinic acid	5.7548E-6	2.4170E-4	3.1090E-1
Arginine biosynthesis		3/14	L-glutamic acid, L-ornithine, L-glutamine	3.3204E-4	9.2972E-3	1.7766E-1
Arginine and proline metabolism		4/38	Hydroxyproline, L-proline, L-glutamic acid, L-ornithine	5.0173E-4	1.0536E-2	3.3542E-1
D-Glutamine and D-glutamate metabolism		2/6	L-glutamic acid, L-glutamine	1.5432E-3	2.1605E-2	5.0000E-1
Glutathione metabolism		2/28	L-glutamic acid, L-ornithine	3.3941E-2	3.1678E-1	1.9660E-2
Phenylalanine, tyrosine and tryptophan biosynthesis		1/4	L-phenylalanine	4.1783E-2	3.5098E-1	5.0000E-1
Butanoate metabolism	Liver	4/15	(R)− 3-Hydroxybutanoate, 4-Aminobutanoate, L-glutamic acid, Succinate	3.4354E-5	2.8857E-3	3.175E-2
Glutathione metabolism		3/28	Glycine, L-glutamic acid, Cadaverine	6.0881E-3	1.2785E-1	1.0839E-1
Alanine, aspartate and glutamate metabolism		3/28	4-Aminobutanoate, L-glutamic acid, Succinate	6.0881E-3	1.2785E-1	2.8366E-1
Phenylalanine, tyrosine and tryptophan biosynthesis	Kidney	2/4	L-phenylalanine, L-tyrosine	7.077E-4	2.9723E-2	1.0000E+ 0
Phenylalanine metabolism		2/12	L-phenylalanine, L-tyrosine	7.3816E-3	1.5501E-1	3.5714E-1
Glutathione metabolism		2/28	L-cysteine, Pyroglutamic acid	3.8030E-2	6.3891E-1	1.052E-2
Glyoxylate and dicarboxylate metabolism	Heart	5/32	Cis-aconitic acid, Citrate, L-serine, L-glutamic acid, L-glutamine	6.3350E-5	5.3214E-3	9.7890E-2
Alanine, aspartate and glutamate metabolism		4/28	L-aspartate, L-glutamic acid, L-glutamine, Citrate	5.5239E-4	1.5467E-2	5.3446E-1
Arginine biosynthesis		3/14	L-aspartate, L-glutamic acid, L-glutamine	8.8344E-4	1.8552E-2	1.1675E-1
D-Glutamine and D-glutamate metabolism		2/6	L-glutamic acid, L-glutamine	2.9391E-3	4.1148E-2	5.0000E-1
Pantothenate and CoA biosynthesis		2/19	Pantothenate, L-aspartate	2.9873E-2	2.7527E-1	7.1400E-3
Citrate cycle (TCA cycle)		2/20	Cis-aconitic acid, Citrate	3.2901E-2	2.7527E-1	1.4041E-1
Nicotinate and nicotinamide metabolism	Hippocampus	2/15	L-aspartate, Nicotinamide	2.0691E-2	4.3450E-1	1.9430E-1
Pantothenate and CoA biosynthesis		2/19	L-aspartate, Beta-alanine	3.2474E-2	5.4556E-1	2.1430E-2
beta-Alanine metabolism		2/21	Beta-alanine, L-aspartate	3.9152E-2	5.4813E-1	3.9925E-1
Pantothenate and CoA biosynthesis	Cortex	2/19	Pantothenate, L-valine	9.1995E-3	1.9319E-1	7.1400E-3
Alanine, aspartate and glutamate metabolism		2/28	N-acetyl-L-aspartic acid, L-alanine	1.9541E-2	3.2830E-1	8.6540E-2
Phenylalanine, tyrosine and tryptophan biosynthesis		1/4	L-phenylalanine	3.1463E-2	4.4048E-1	5.0000E-1
Linoleic acid metabolism		1/5	Linoleate	3.9185E-2	4.7022E-1	1.0000E+ 1
Glutathione metabolism	Kidney fat	2/28	Glycine, 5-oxoproline	4.7583E-3	1.9985E-1	9.5820E-2
Primary bile acid biosynthesis		2/46	Cholesterol, Glycine	1.2616E-2	3.5325E-1	5.5630E-2
Alanine, aspartate and glutamate metabolism	Brown fat	3/28	L-alanine, L-glutamic acid, Citrate	8.5565E-4	5.3543E-2	1.9712E-1
Glyoxylate and dicarboxylate metabolism		3/32	Citrate, Glycine, L-glutamic acid	1.2748E-3	5.3543E-2	1.3757E-1
Glutathione metabolism		2/28	Glycine, L-glutamic acid	1.6472E-2	3.1593E-1	1.0839E-1
Primary bile acid biosynthesis		2/46	Cholesterol, Glycine	4.1980E-2	4.5169E-1	5.5630E-2
D-Glutamine and D-glutamate metabolism		1/6	L-glutamic acid	4.3018E-2	4.5169E-1	5.0000E-1

Raw p, the original p value calculated from the enrichment analysis; FDR, false discovery rate.

organs. The liver, the body's main metabolic organ, is a soft tissue sensitive to fluorosis. Animal experiments have confirmed that excessive intake of fluoride can cause abnormalities in the structure and function of liver (Pereira et al., 2018). The volume of fatty acids in the liver of rats exposed to fluoride increased significantly, including arachidonic acid, stearic acid, linoleic acid, oleic acid, vaccenic acid, and palmitic acid. Free fatty acid is the main mediator of hepatic steatosis. Patients with non-alcoholic fatty liver disease commonly have elevated fatty acid levels (Vergani, 2019). High levels of arachidonic acid, linoleic acid and their derivatives may be closely related to inflammation (Buckley et al., 2014). Arachidonic acid is the precursor of many pro-inflammatory substances and mediates the production of inflammatory cytokines

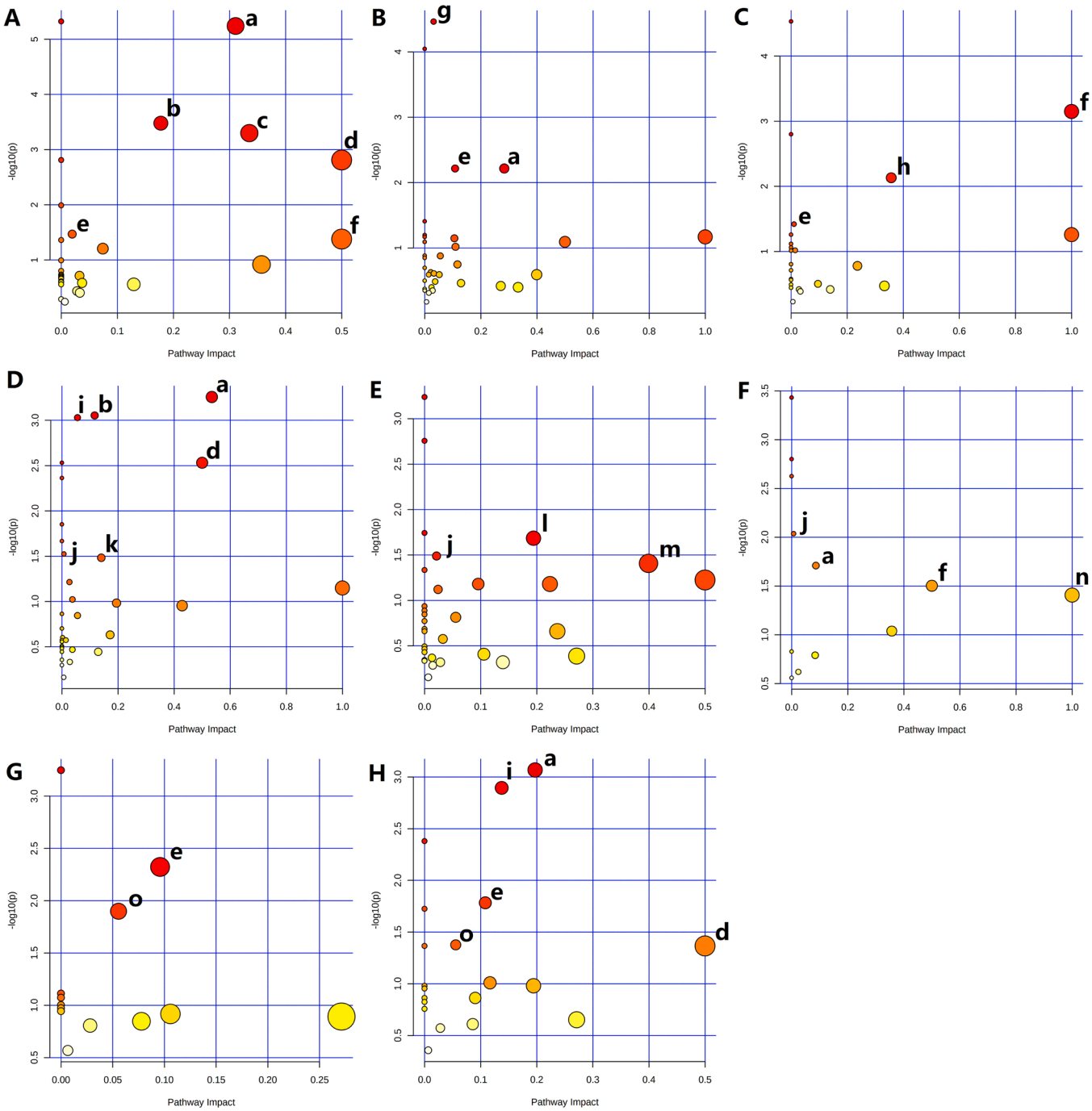

Fig. 4. Pathway analysis diagram of (A) serum, (B) liver, (C) kidney, (D) heart, (E) hippocampus, (F) cortex, (G) kidney fat, and (H) brown fat performed using MetaboAnalyst 5.0. (a) Alanine, aspartate and glutamate metabolism; (b) arginine biosynthesis; (c) arginine and proline metabolism; (d) D-glutamine and D-glutamate metabolism; (e) glutathione metabolism; (f) phenylalanine, tyrosine and tryptophan biosynthesis; (g) butanoate metabolism; (h) phenylalanine metabolism; (i) glyoxylate and dicarboxylate metabolism; (j) pantothenate and CoA biosynthesis; (k) citrate cycle (TCA cycle); (l) nicotinate and nicotinamide metabolism; (m) beta-zlanine metabolism; (n) linoleic acid metabolism; (o) primary bile acid biosynthesis.

(Korotkova and Lundberg, 2014). The increase of palmitic acid content may lead to a toxic effect on hepatocytes (Joshi-Barve et al., 2007). Palmitic acid can cause oxidative stress by destroying the mitochondrial respiratory chain. Studies have shown that palmitic acid can activate endoplasmic reticulum stress, and induce tissue inflammation and insulin resistance (Lu et al., 2013). Animal experiments showed that fluorine can cause lipid peroxidation damage in the liver, generate a large number of free radicals and lipid peroxide, and affect the normal functions of cell membrane structural proteins, membrane transport proteins, receptor proteins, and contact channel proteins, resulting in abnormal cell membrane biological functions and damage to biological macromolecules (Zhao et al., 2018; Zhou et al., 2015). Therefore, inflammation and oxidative stress may be the mechanisms of hepatotoxicity arising from fluoride exposure.

Fluoride exposure also changed the level of amino acids in the liver of rats. Compared with the control group, the level of glycine in the liver of rats exposed to fluoride decreased. Glycine may have a significant hepatoprotective effect which can protect liver parenchymal cells and sinusoidal endothelial cells (Qu et al., 2002; Zhang et al., 2000; Zhong et al., 1996). The abnormal increase of beta-alanine in the liver may

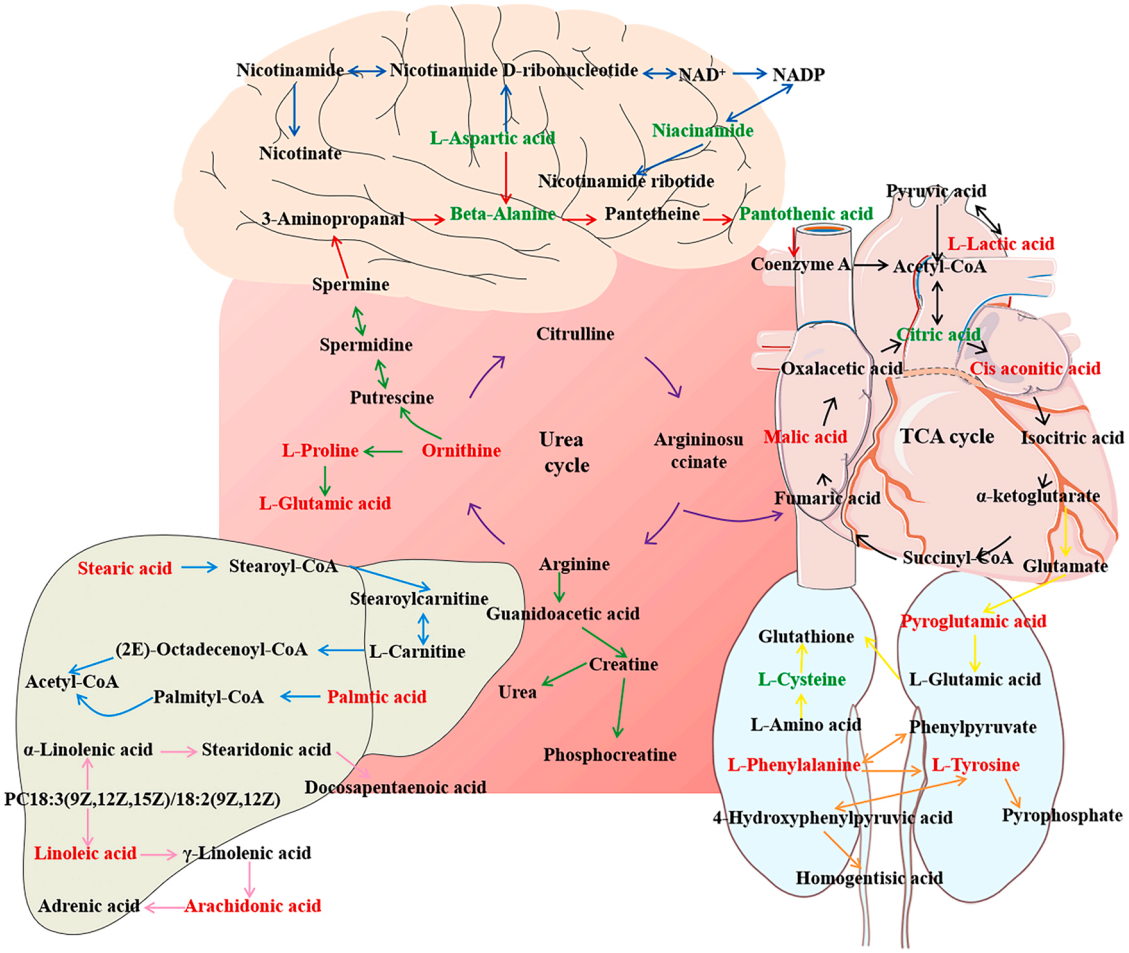

Fig. 5. Metabolic pathways of major organs affected by fluoride processing (black arrows indicate energy metabolism pathways, including TCA cycle and glycolysis; purple arrows indicate the urea cycle; red arrows indicate beta-alanine metabolism; blue arrows indicate nicotinate and nicotinamide metabolism; green arrows indicate arginine and proline metabolism; yellow arrows indicate glutathione metabolism; pink arrows indicate arachidonic acid metabolism; orange arrows indicate phenylalanine metabolism; light blue arrows indicate fatty acid metabolism). Metabolites marked in red indicate upregulation of metabolite levels due to fluoride exposure, and downregulated metabolite levels are marked in green.

have adverse effects on liver cells. High levels of alanine may confer mitochondrial toxicity and metabolic toxicity. Alanine can reduce the level of taurine in liver cells, and taurine plays an important role in maintaining mitochondrial respiratory function and reducing the production of superoxide (Shetewy et al., 2016). In addition to its neurotoxicity, gamma-aminobutyric acid, a metabolic toxin, can also adversely affect the body when present at high levels (Ikegami et al., 2018).

4.3. Kidney metabolism analysis

The kidney is the main excretion route of sodium fluoride. At a high concentration, sodium fluoride will target the kidney, especially the proximal tubular epithelial cells, resulting in renal injury (Wahluyo et al., 2017). The mechanism may involve oxidative stress and energy metabolism disorders. Metabolomics results showed that the content of L-aspartic acid in the kidney decreased, the levels of pyroglutamic acid and L-cysteine changed, and the level of glutathione metabolism decreased in the fluoride exposed group. L-aspartic acid is the precursor of cell signaling compounds, and is also a metabolite in the urea cycle and participates in gluconeogenesis. In addition, aspartic acid carries a reducing equivalent in the mitochondrial malate-aspartic acid shuttle, which plays an important role in the glycolysis process (Altinok et al., 2020). The reduction of its content may inhibit the glycolysis process, thereby causing renal metabolic disorders and affecting signal transduction. Metabolic pathway analysis showed that the glutathione metabolism pathway in the kidney was affected. Glutathione is the main antioxidant in the body. It has antioxidant effects and integrated detoxification effects (Wu et al., 2004). On the one hand, as an important antioxidant in the body, it can remove free radicals. On the other hand, it participates in biotransformation so as to convert harmful poisons into harmless substances and excrete them from the body (Sies, 1999). Pyroglutamic acid is a cyclized derivative of L-glutamic acid, which can be used as an acidogen and metabotoxin. Long term high levels of pyroglutamic acid may lead to metabolic acidosis (Luyasu et al., 2014). The increase in the level of pyroglutamic acid may be related to the abnormal metabolism of glutathione. Cysteine is very important in energy metabolism. It is a structural component of many tissues and hormones, a precursor of protein synthesis, and an antioxidant. In the body, cysteine can produce glutathione (Paul et al., 2018). Studies showed that sodium fluoride significantly decreased the activity and total antioxidant capacity of antioxidant enzymes (glutathione peroxidase and superoxide dismutase), increased lipid peroxidation, and increased cell apoptosis (Lu et al., 2017). In addition, an increase in the content of the toxic substance ethylamine in the kidney was detected, which may also be one of the causes of kidney damage caused by sodium fluoride.

4.4. Heart metabolism analysis

Fluoride may cause cardiotoxicity, and an increased probability of heart disease and its complications was observed in fluorosis endemic areas (Adali et al., 2013). Myocardial damage caused by fluorosis may be caused by oxidative stress, lipid peroxidation, inflammation, and metabolic disorders (Quadri et al., 2018). In the heart tissue, the levels of L-serine, L-glutamine, L-aspartic acid, and L-glutamic acid in fluoride-exposed rats were reduced. Metabolic pathway analysis showed that the heart related arginine synthesis pathway and tricarboxylic acid circulation pathway were disordered. These changes may affect the physiological function of the heart and induce cardiomyocyte apoptosis. L-glutamine plays an important role in cardiovascular physiology and pathology (Durante, 2019). As a donor in protein and nucleic acid synthesis, glutamine can participate in important activities in heart and vascular cells, maintain the concentration of glutamic acid and adenosine triphosphate, and protect cardiomyocytes from oxidative stress by inducing the synthesis of GSH (Watanabe et al., 2021). Glutamine can enhance the activity of antioxidants by inducing the expression of heat shock proteins, balance the expression of pro-inflammatory factors and anti-inflammatory factors, have an important anti-inflammatory and antioxidant effect in the circulatory system, improve myocardial energy supply and cellular energy metabolism, and prevent the accumulation of lactic acid in myocardial cells (Wischmeyer, 2002). The decrease of L-glutamine and L-glutamic acid content and the increase of L-lactic acid levels have indicated that the heart has suffered oxidative stress damage and energy metabolism disorders.

Citric acid and cis-aconitic acid are important components of the tricarboxylic acid cycle, and participate in the common metabolic pathways of carbohydrate, fat, and protein. The changes in their levels indicated that the tricarboxylic acid cycle was disturbed. Therefore, fluoride exposure may lead to mitochondrial damage. This conclusion has been confirmed by other studies (Wang et al., 2020). In addition, citric acid can reduce lipid peroxidation and inflammation and have a cardioprotective effect (Abdel-Salam et al., 2014). The synthesis and metabolism of arginine in the fluoride exposed group were also disturbed. Arginine is not only an important raw material for protein synthesis, but also a precursor for the synthesis of creatine, polyamine, and nitric oxide (NO) in the body. Arginine plays an important regulatory role in the prevention and treatment of cardiovascular diseases, and in reducing common cardiovascular dysfunction caused by coronary heart disease, ischemic injury, and heart failure (Wu and Meininger, 2000). NO can also control platelet aggregation and regulate cardiac contractility. These effects are mediated by the activation of soluble guanylate cyclase, which in turn increases the concentration of cGMP in target cells (Sudar-Milovanovic et al., 2016).

4.5. Brain metabolism analysis

Sodium fluoride is neurotoxic and can cause damage to the brain and nervous system because it can penetrate the blood-brain barrier. Fluoride exposure may lead to brain metabolism disorders. In this study, metabolites in the hippocampus and cortex were detected, and the results showed that the levels of various amino acids changed. The content of glycine and L-lysine in the hippocampus of rats exposed to fluoride decreased significantly. Glycine is the simplest amino acid in the body and can participate in signal transmission as a neurotransmitter in the central nervous system (Rajendra et al., 1997). Hippocampal glycine signal dysfunction is related to neuropsychiatric disorders. Glycine is a constituent amino acid of GSH, which can inhibit the formation of reactive oxygen species (ROS) and reduce the occurrence of oxygen stress. It also has broad-spectrum anti-inflammatory, cell protection, and immune regulation effects (Weinberg et al., 1987). The disorder of glycine metabolism may be related to oxidative stress in brain tissue. As an essential amino acid, lysine is involved in the synthesis of various proteins such as skeletal muscle, enzymes, serum proteins, and peptide hormones in the body. Low lysine levels have been found in patients with Parkinson's disease, asthma, kidney disease, hypothyroidism, and depression (Barbot et al., 1997; Engelborghs et al., 2003; Ntontsi et al., 2020).

Fluoride exposure affected the metabolism of nicotinate and nicotinamide in the rat brain. Nicotinamide is the amide form of nicotinic acid, which is the precursor for the synthesis of coenzyme I and coenzyme II (Rennie et al., 2015). By participating in cell energy metabolism, it plays a protective role during oxidative stress or inflammatory damage, effectively preventing cells and cell membranes from free radical damage, and is closely related to metabolic processes such as glycolysis, pyruvate metabolism and fatty acid metabolism (Li et al., 2006; Maiese et al., 2009). Fluoride exposure also affects the synthesis pathways of pantothenic acid and coenzyme A (CoA) in the hippocampus and cortex. Pantothenic acid is an important part of the synthesis of CoA, which is a key cofactor involved in many pathways including fatty acid biosynthesis and the tricarboxylic acid cycle, and plays a role in transferring acyl groups in metabolism (Tahiliani and Beinlich, 1991). CoA is involved in the synthesis of many important substances in the brain, such as acetylcholine, neuromuscular messengers, and melatonin. In pantothenic acid deficiency, the oxidation of fatty acids is inhibited and may induce brain damage.

Our study systematically studied changes of metabolites in the whole body and main organs of rats under fluoride exposure through metabolomics methods. These findings can be used to speculate on potential biomarkers or the possible toxicity mechanism of fluorosis. However, while GC-MS technology can detect most of the metabolites in the body, there are still certain limitations, although detection can be improved by also using nuclear magnetic resonance and liquid chromatography-mass spectrometry. In addition, this study lacked examination of the dose response relationship, and used a single metabolomics method. However, the single metabolomics method can be set dose groups or combined with proteomics, genomics and other multiple omics methods to further verify our findings in the future.

5. Conclusion

In our study, metabolomics methods were used to screen out the differential metabolites in the serum and major organs of fluoride exposed rats, and the metabolic pathways affected by fluoride exposure were analyzed. Proline, ornithine, etc. can be used as potential biomarkers of fluorosis. The mechanisms of fluoride damage to different organs may include oxidative stress, inflammation, mitochondrial damage, fatty acid, amino acid, and energy metabolism disorders. This study deepens the understanding of the toxicity mechanism of sodium fluoride and provides new avenues for the diagnosis and prevention of fluorosis.

CRediT authorship contribution statement

Shiyuan Zhao: Conceptualization, Methodology, Data Curation, Writing-Original Draft. **JinXiu Guo:** Validation, Investigation, Visualization, Data Curation. **Hongjia Xue:** Investigation, Data Curation. **Junjun Meng:** Resources, Investigation, Writing - Review & Editing. **Dadi Xie:** Writing - Review & Editing, Visualization. **Xi Liu:** Formal analysis. **Qingqing Yu:** Validation. **Haitao Zhong:** Resources, Investigation.**Pei Jiang:** Resources, Supervision, Project administration, Funding acquisition.

Declaration of Competing Interest

The authors declare that they have no known competing financial interests or personal relationships that could have appeared to influence the work reported in this paper.

Acknowledgments

This work was supported by the National Natural Science Foundation of China (no. 81602846), the Natural Science Foundation of Shandong Province (no. ZR2021MH145) and the Taishan Scholar Project of Shandong Province (no. tsqn201812159).

Appendix A. Supporting information

Supplementary data associated with this article can be found in the online version at doi:10.1016/j.ecoenv.2022.113888.

References

Abdel-Salam, O.M., Youness, E.R., Mohammed, N.A., Morsy, S.M., Omara, E.A., Sleem, A.A., 2014. Citric acid effects on brain and liver oxidative stress in lipopolysaccharide-treated mice. J. Med. Food 17 (5), 588–598. https://doi.org/10.1089/jmf.2013.0065.

Adali, M.K., Varol, E., Aksoy, F., Icli, A., Ersoy, I.H., Ozaydin, M., Erdogan, D., Dogan, A., 2013. Impaired heart rate recovery in patients with endemic fluorosis. Biol. Trace Elem. Res. 152 (3), 310–315. https://doi.org/10.1007/s12011-013-9627-6.

Agalakova, N.I., Nadei, O.V., 2020. Inorganic fluoride and functions of brain. Crit. Rev. Toxicol. 50 (1), 28–46. https://doi.org/10.1080/10408444.2020.1722061.

Altinok, O., Poggio, J.L., Stein, D.E., Bowne, W.B., Shieh, A.C., Snyder, N.W., Orynbayeva, Z., 2020. Malate-aspartate shuttle promotes l-lactate oxidation in mitochondria. J. Cell. Physiol. 235 (3), 2569–2581. https://doi.org/10.1002/jcp.29160.

Barbot, C., Fineza, I., Diogo, L., Maia, M., Melo, J., Guimarães, A., Pires, M.M., Cardoso, M.L., Vilarinho, L., 1997. L-2-hydroxyglutaric aciduria: clinical, biochemical and magnetic resonance imaging in six Portuguese pediatric patients. Brain Dev. 19 (4), 268–273. https://doi.org/10.1016/s0387-7604(97)00574-3.

Buckley, C.D., Gilroy, D.W., Serhan, C.N., 2014. Proresolving lipid mediators and mechanisms in the resolution of acute inflammation. Immunity 40 (3), 315–327. https://doi.org/10.1016/j.immuni.2014.02.009.

Buzalaf, M.A.R., Whitford, G.M., 2011. Fluoride metabolism. Monogr. Oral Sci. 22, 20–36. https://doi.org/10.1159/000325107.

Chatterjee, P., Cheong, Y.J., Bhatnagar, A., et al., 2021. Plasma metabolites associated with biomarker evidence of neurodegeneration in cognitively normal older adults. J. Neurochem. 59 (2), 389–402. https://doi.org/10.1111/jnc.15128.

De la Fuente, B., Vázquez, M., Rocha, R.A., Devesa, V., Vélez, D., 2016. Effects of sodium fluoride on immune response in murine macrophages. Toxicol. Vitr. 34, 81–87. https://doi.org/10.1016/j.tiv.2016.03.001.

DenBesten, P., Li, W., 2011. Chronic fluoride toxicity: dental fluorosis. Monogr. Oral Sci. 22, 81–96. https://doi.org/10.1159/000327028.

Dharmaratne, R.W., 2019. Exploring the role of excess fluoride in chronic kidney disease: a review. Hum. Exp. Toxicol. 38 (3), 269–279. https://doi.org/10.1177/0960327118814161.

Dunn, W.B., Wilson, I.D., Nicholls, A.W., Broadhurst, D., 2012. The importance of experimental design and QC samples in large-scale and MS-driven untargeted metabolomic studies of humans. Bioanalysis 4 (18), 2249–2264. https://doi.org/10.4155/bio.12.204.

Durante, W., 2019. The emerging role of l-glutamine in cardiovascular health and disease. Nutrients 11 (9), 2092. https://doi.org/10.3390/nu11092092.

Engelborghs, S., Marescau, B., De Deyn, P.P., 2003. Amino acids and biogenic amines in cerebrospinal fluid of patients with Parkinson's disease. Neurochem. Res. 28 (8), 1145–1150. https://doi.org/10.1023/a:1024255208563.

Faibish, D., Suzuki, M., Bartlett, J.D., 2016. Appropriate real-time PCR reference genes for fluoride treatment studies performed in vitro or in vivo. Arch. Oral Biol. 62, 33–42. https://doi.org/10.1016/j.archoralbio.2015.11.004.

Fonteh, A.N., Harrington, R.J., Tsai, A., Liao, P., Harrington, M.G., 2007. Free amino acid and dipeptide changes in the body fluids from Alzheimer's disease subjects. Amino Acids 32 (2), 213–224. https://doi.org/10.1007/s00726-006-0409-8.

Guissouma, W., Hakami, O., Al-Rajab, A.J., Tarhouni, J., 2017. Risk assessment of fluoride exposure in drinking water of Tunisia. Chemosphere 177, 102–108. https://doi.org/10.1016/j.chemosphere.2017.03.011.

Gupta, R.S., Khan, T.I., Agrawal, D., Kachhawa, J.B., 2007. The toxic effects of sodium fluoride on the reproductive system of male rats. Toxicol. Ind. Health 23 (9), 507–513. https://doi.org/10.1177/0748233708089041.

Ikegami, R., Shimizu, I., Sato, T., Yoshida, Y., Hayashi, Y., Suda, M., Katsuumi, G., Li, J., Wakasugi, T., Minokoshi, Y., Okamoto, S., Hinoi, E., Nielsen, S., Jespersen, N.Z., Scheele, C., Soga, T., Minamino, T., 2018. Gamma-aminobutyric acid signaling in brown adipose tissue promotes systemic metabolic derangement in obesity. Cell Rep. 24 (11), 2827–2837.e5. https://doi.org/10.1016/j.celrep.2018.08.024.

Jha, S.K., Mishra, V.K., Sharma, D.K., Damodaran, T., 2011. Fluoride in the environment and its metabolism in humans. Rev. Environ. Contam. Toxicol. 211, 121–142. https://doi.org/10.1007/978-1-4419-8011-3_4.

Jiang, P., Li, G., Zhou, X., Wang, C., Qiao, Y., Liao, D., Shi, D., 2019. Chronic fluoride exposure induces neuronal apoptosis and impairs neurogenesis and synaptic plasticity: role of GSK-3β/β-catenin pathway. Chemosphere 214, 430–435. https://doi.org/10.1016/j.chemosphere.2018.09.095.

Johnson, C.H., Ivanisevic, J., Siuzdak, G., 2016. Metabolomics: beyond biomarkers and towards mechanisms. Nat. Rev. Mol. Cell Biol. 17 (7), 451–459. https://doi.org/10.1038/nrm.2016.25.

Joshi-Barve, S., Barve, S.S., Amancherla, K., Gobejishvili, L., Hill, D., Cave, M., Hote, P., McClain, C.J., 2007. Palmitic acid induces production of proinflammatory cytokine interleukin-8 from hepatocytes. Hepatology 46 (3), 823–830. https://doi.org/10.1002/hep.21752.

Karna, E., Szoka, L., Huynh, T.Y.L., Palka, J.A., 2020. Proline-dependent regulation of collagen metabolism. Cell Mol. Life Sci. 77 (10), 1911–1918. https://doi.org/10.1007/s00018-019-03363-3.

Kheradpisheh, Z., Mirzaei, M., Mahvi, A.H., Mokhtari, M., Azizi, R., Fallahzadeh, H., Ehrampoush, M.H., 2018. Impact of drinking water fluoride on human thyroid hormones: a case- control study. Sci. Rep. 8 (1), 2674. https://doi.org/10.1038/s41598-018-20696-4.

Korotkova, M., Lundberg, I.E., 2014. The skeletal muscle arachidonic acid cascade in health and inflammatory disease. Nat. Rev. Rheumatol. 10 (5), 295–303. https://doi.org/10.1038/nrrheum.2014.2.

Kumar, J., Haldar, C., Verma, R., 2020. Fluoride compromises testicular redox sensor, gap junction protein, and metabolic status: amelioration by melatonin. Biol. Trace Elem. Res 196 (2), 552–564. https://doi.org/10.1007/s12011-019-01946-6.

Li, F., Chong, Z.Z., Maiese, K., 2006. Cell life versus cell longevity: the mysteries surrounding the NAD+ precursor nicotinamide. Curr. Med. Chem. 13 (8), 883–895. https://doi.org/10.2174/092986706776361058.

Li, L., Lin, L.M., Deng, J., Lin, X.L., Li, Y.M., Xia, B.H., 2021. The therapeutic effects of Prunella vulgaris against fluoride-induced oxidative damage by using the metabolomics method. Environ. Toxicol. 36 (9), 1802–1816. https://doi.org/10.1002/tox.23301.

Li, P., Wu, G., 2018. Roles of dietary glycine, proline, and hydroxyproline in collagen synthesis and animal growth. Amino Acids 50 (1), 29–38. https://doi.org/10.1007/s00726-017-2490-6.

Lu, Y., Qian, L., Zhang, Q., Chen, B., Gui, L., Huang, D., Chen, G., Chen, L., 2013. Palmitate induces apoptosis in mouse aortic endothelial cells and endothelial dysfunction in mice fed high-calorie and high-cholesterol diets. Life Sci. 92 (24–26), 1165–1173. https://doi.org/10.1016/j.lfs.2013.05.002.

Lu, Y., Luo, Q., Cui, H., Deng, H., Kuang, P., Liu, H., Fang, J., Zuo, Z., Deng, J., Li, Y., Wang, X., Zhao, L., 2017. Sodium fluoride causes oxidative stress and apoptosis in the mouse liver. Aging 9 (6), 1623–1639. https://doi.org/10.18632/aging.101257.

Luyasu, S., Wamelink, M.M., Galanti, L., Dive, A., 2014. Pyroglutamic acid-induced metabolic acidosis: a case report. Acta Clin. Belg. 69 (3), 221–223. https://doi.org/10.1179/2295333714Y.0000000022.

Maiese, K., Chong, Z.Z., Hou, J., Shang, Y.C., 2009. The vitamin nicotinamide: translating nutrition into clinical care. Molecules 14 (9), 3446–3485. https://doi.org/10.3390/molecules14093446.

Malin, A.J., Lesseur, C., Busgang, S.A., Curtin, P., Wright, R.O., Sanders, A.P., 2019. Fluoride exposure and kidney and liver function among adolescents in the United States: NHANES, 2013-2016. Environ. Int. 132, 105012 https://doi.org/10.1016/j.envint.2019.105012.

McGill, P.E., 1995. Endemic fluorosis. Baillieres Clin. Rheumatol. 9 (1), 75–81. https://doi.org/10.1016/s0950-3579(05)80145-1.

Moimaz, S.A., Saliba, O., Marques, L.B., Garbin, C.A., Saliba, N.A., 2015. Dental fluorosis and its influence on children's life. Braz. Oral Res. 29 (1), 1–7. https://doi.org/10.1590/1807-3107BOR-2015.vol29.0014.

Nadler, J.V., Wang, A., Hakim, A., 1988. Toxicity of L-proline toward rat hippocampal neurons. Brain Res. 456 (1), 168–172. https://doi.org/10.1016/0006-8993(88)90358-7.

Ni, Y., Xie, G., Jia, W., 2014. Metabonomics of human colorectal cancer: new approaches for early diagnosis and biomarker discovery. J. Proteome Res. 13 (9), 3857–3870. https://doi.org/10.1021/pr500443c.

Niu, R., Chen, H., Manthari, R.K., Sun, Z., Wang, J., Zhang, J., Wang, J., 2018. Effects of fluoride on synapse morphology and myelin damage in mouse hippocampus. Chemosphere 194, 628–633. https://doi.org/10.1016/j.chemosphere.2017.12.027.

Ntontsi, P., Ntzoumanika, V., Loukides, S., Benaki, D., Gkikas, E., Mikros, E., Bakakos, P., 2020. EBC metabolomics for asthma severity. J. Breath. Res. 14 (3), 036007 https://doi.org/10.1088/1752-7163/ab9220.

Panneerselvam, L., Raghunath, A., Sundarraj, K., Perumal, E., 2019. Acute fluoride exposure alters myocardial redox and inflammatory markers in rats. Mol. Biol. Rep. 46 (6), 6155–6164. https://doi.org/10.1007/s11033-019-05050-9.

Papadimitropoulos, M.P., Vasilopoulou, C.G., Maga-Nteve, C., Klapa, M.I., 2018. Untargeted GC-MS metabolomics. Methods Mol. Biol. 1738, 133–147. https://doi.org/10.1007/978-1-4939-7643-0_9.

Patil, M.M., Lakhkar, B.B., Patil, S.S., 2018. Curse of fluorosis. Indian J. Pediatr. 85 (5), 375–383. https://doi.org/10.1007/s12098-017-2574-z.

Paul, B.D., Sbodio, J.I., Snyder, S.H., 2018. Cysteine metabolism in neuronal redox homeostasis. Trends Pharm. Sci. 39 (5), 513–524. https://doi.org/10.1016/j.tips.2018.02.007.

Pereira, H.A.B.D.S., Dionizio, A.S., Araujo, T.T., Fernandes, M.D.S., Iano, F.G., Buzalaf, M.A.R., 2018. Proposed mechanism for understanding the dose- and time-dependency of the effects of fluoride in the liver. Toxicol. Appl. Pharm. 358, 68–75. https://doi.org/10.1016/j.taap.2018.09.010.

Phang, J.M., 2019. Proline metabolism in cell regulation and cancer biology: recent advances and hypotheses. Antioxid. Redox Signal. 30 (4), 635–649. https://doi.org/10.1089/ars.2017.7350.

Qing-Feng, S., Ying-Peng, X., Tian-Tong, X., 2019. Matrix metalloproteinase-9 and p53 involved in chronic fluorosis induced blood-brain barrier damage and neurocyte changes. Arch. Med. Sci. 15 (2), 457–466. https://doi.org/10.5114/aoms.2019.83294.

Qu, W., Ikejima, K., Zhong, Z., Waalkes, M.P., Thurman, R.G., 2002. Glycine blocks the increase in intracellular free Ca2+ due to vasoactive mediators in hepatic parenchymal cells. Am. J. Physiol. Gastrointest. Liver Physiol. 283 (6), G1249–G1256. https://doi.org/10.1152/ajpgi.00197.2002.

Quadri, J.A., Sarwar, S., Pinky, Kar, P., Singh, S., Mallick, S.R., Arava, S., Nag, T.C., Roy, T.S., Shariff, A., 2018. Fluoride induced tissue hypercalcemia, IL-17 mediated inflammation and apoptosis lead to cardiomyopathy: ultrastructural and biochemical findings. Toxicology 406–407, 44–57. https://doi.org/10.1016/j.tox.2018.05.012.

Rajendra, S., Lynch, J.W., Schofield, P.R., 1997. The glycine receptor. Pharm. Ther. 73 (2), 121–146. https://doi.org/10.1016/s0163-7258(96)00163-5.

Rennie, G., Chen, A.C., Dhillon, H., Vardy, J., Damian, D.L., 2015. Nicotinamide and neurocognitive function. Nutr. Neurosci. 18 (5), 193–200. https://doi.org/10.1179/1476830514Y.0000000112.

Saeed, M., Malik, R.N., Kamal, A., 2020. Fluorosis and cognitive development among children (6-14 years of age) in the endemic areas of the world: a review and critical analysis. Environ. Sci. Pollut. Res. Int. 27 (3), 2566–2579. https://doi.org/10.1007/s11356-019-06938-6.

Salvi, S., Santorelli, F.M., Bertini, E., Boldrini, R., Meli, C., Donati, A., Burlina, A.B., Rizzo, C., Di Capua, M., Fariello, G., Dionisi-Vici, C., 2001. Clinical and molecular findings in hyperornithinemia-hyperammonemia-homocitrullinuria syndrome. Neurology 57 (5), 911–914. https://doi.org/10.1212/wnl.57.5.911.

Sellami, M., Riahi, H., Maatallah, K., Ferjani, H., Bouaziz, M.C., Ladeb, M.F., 2020. Skeletal fluorosis: don't miss the diagnosis! Skelet. Radiol. 49 (3), 345–357. https://doi.org/10.1007/s00256-019-03302-0.

Shetewy, A., Shimada-Takaura, K., Warner, D., Jong, C.J., Mehdi, A.B., Alexeyev, M., Takahashi, K., Schaffer, S.W., 2016. Mitochondrial defects associated with β-alanine toxicity: relevance to hyper-beta-alaninemia. Mol. Cell Biochem. 416 (1–2), 11–22. https://doi.org/10.1007/s11010-016-2688-z.

Sies, H., 1999. Glutathione and its role in cellular functions. Free Radic. Biol. Med. 27 (9–10), 916–921. https://doi.org/10.1016/s0891-5849(99)00177-x.

Simell, O., Takki, K., 1973. Raised plasma-ornithine and gyrate atrophy of the choroid and retina. Lancet 1 (7811), 1031–1033. https://doi.org/10.1016/s0140-6736(73)90667-3.

Singh, G., Kumari, B., Sinam, G., Kriti, Kumar, N., Mallick, S., 2018. Fluoride distribution and contamination in the water, soil and plants continuum and its remedial technologies, an Indian perspective – a review. Environ. Pollut. 239, 95–108. https://doi.org/10.1016/j.envpol.2018.04.002.

Srivastava, S., Flora, S.J.S., 2020. Fluoride in drinking water and skeletal fluorosis: a review of the global impact. Curr. Environ. Health Rep. 7 (2), 140–146. https://doi.org/10.1007/s40572-020-00270-9.

Staufner, C., Haack, T.B., Feyh, P., Gramer, G., Raga, D.E., Terrile, C., Sauer, S., Okun, J. G., Fang-Hoffmann, J., Mayatepek, E., Prokisch, H., Hoffmann, G.F., Kölker, S., 2016. Genetic cause and prevalence of hydroxyprolinemia. J. Inherit. Metab. Dis. 39 (5), 625–632. https://doi.org/10.1007/s10545-016-9940-2.

Sudar-Milovanovic, E., Obradovic, M., Jovanovic, A., Zaric, B., Zafirovic, S., Panic, A., Radak, D., Isenovic, E.R., 2016. Benefits of L-arginine on cardiovascular system. Mini Rev. Med. Chem. 16 (2), 94–103. https://doi.org/10.2174/1389557515666151016125826.

Suzuki, M., Bartlett, J.D., 2014. Sirtuin1 and autophagy protect cells from fluoride-induced cell stress. Biochim. Biophys. Acta 1842 (2), 245–255. https://doi.org/10.1016/j.bbadis.2013.11.023.

Suzuki, M., Bandoski, C., Bartlett, J.D., 2015. Fluoride induces oxidative damage and SIRT1/autophagy through ROS-mediated JNK signaling. Free Radic. Biol. Med. 89, 369–378. https://doi.org/10.1016/j.freeradbiomed.2015.08.015.

Tahiliani, A.G., Beinlich, C.J., 1991. Pantothenic acid in health and disease. Vitam. Horm. 46, 165–228. https://doi.org/10.1016/s0083-6729(08)60684-6.

Vergani, L., 2019. Fatty acids and effects on in vitro and in vivo models of liver steatosis. Curr. Med. Chem. 26, 3439–3456. https://doi.org/10.2174/0929867324666170518101334.

Wahluyo, S., Ismiyatin, K., Purwanto, B., Mukono, I.S., 2017. The influence of sodium fluoride on the growth of ameloblasts and kidney proximal tubular cells. Folia Biol. 63 (1), 31–34.

Wang, H.W., Liu, J., Wei, S.S., Zhao, W.P., Zhu, S.Q., Zhou, B.H., 2020. Mitochondrial respiratory chain damage and mitochondrial fusion disorder are involved in liver dysfunction of fluoride-induced mice. Chemosphere 241, 125099. https://doi.org/10.1016/j.chemosphere.2019.125099.

Watanabe, K., Nagao, M., Toh, R., Irino, Y., Shinohara, M., Iino, T., Yoshikawa, S., Tanaka, H., Satomi-Kobayashi, S., Ishida, T., Hirata, K.I., 2021. Critical role of glutamine metabolism in cardiomyocytes under oxidative stress. Biochem. Biophys. Res. Commun. 534, 687–693. https://doi.org/10.1016/j.bbrc.2020.11.018.

Wei, W., Pang, S., Sun, D., 2019. The pathogenesis of endemic fluorosis: research progress in the last 5 years. J. Cell. Mol. Med. 23 (4), 2333–2342. https://doi.org/10.1111/jcmm.14185.

Weinberg, J.M., Davis, J.A., Abarzua, M., Rajan, T., 1987. Cytoprotective effects of glycine and glutathione against hypoxic injury to renal tubules. J. Clin. Investig. 80 (5), 1446–1454. https://doi.org/10.1172/JCI113224.

Whelton, H.P., Spencer, A.J., Do, L.G., Rugg-Gunn, A.J., 2019. Fluoride revolution and dental caries: evolution of policies for global use. J. Dent. Res. 98 (8), 837–846. https://doi.org/10.1177/0022034519843495.

Wischmeyer, P.E., 2002. Glutamine and heat shock protein expression. Nutrition 18 (3), 225–228. https://doi.org/10.1016/s0899-9007(01)00796-1.

Wu, G., Meininger, C.J., 2000. Arginine nutrition and cardiovascular function. J. Nutr. 130 (11), 2626–2629. https://doi.org/10.1093/jn/130.11.2626.

Wu, G., Fang, Y.Z., Yang, S., Lupton, J.R., Turner, N.D., 2004. Glutathione metabolism and its implications for health. J. Nutr. 134 (3), 489–492. https://doi.org/10.1093/jn/134.3.489.

Wu, G., Bazer, F.W., Burghardt, R.C., Johnson, G.A., Kim, S.W., Knabe, D.A., Li, P., Li, X., McKnight, J.R., Satterfield, M.C., Spencer, T.E., 2011. Proline and hydroxyproline metabolism: implications for animal and human nutrition. Amino Acids 40 (4), 1053–1063. https://doi.org/10.1007/s00726-010-0715-z.

Wu, Z., Hou, Y., Dai, Z., Hu, C.A., Wu, G., 2019. Metabolism, nutrition, and redox signaling of hydroxyproline. Antioxid. Redox Signal. 30 (4), 674–682. https://doi.org/10.1089/ars.2017.7338.

Yuan, L., Fei, W., Jia, F., Jun-Ping, L., Qi, L., Fang-Ru, N., Xu-Dong, L., Shu-Lian, X., 2020. Health risk in children to fluoride exposure in a typical endemic fluorosis area on Loess Plateau, north China, in the last decade. Chemosphere 243, 125451. https://doi.org/10.1016/j.chemosphere.2019.125451.

Yue, B., Zhang, X., Li, W., Wang, J., Sun, Z., Niu, R., 2020. Fluoride exposure altered metabolomic profile in rat serum. Chemosphere 258, 127387. https://doi.org/10.1016/j.chemosphere.2020.127387.

Zanglis, A., Andreopoulos, D., Zissimopoulos, A., Baziotis, N., 2005. Positive Tc-99m-MIBI scan in a patient with confirmed Paget's disease of bone. Clin. Nucl. Med. 30 (5), 363–364. https://doi.org/10.1097/01.rlu.0000159911.89757.a6.

Zhang, Y., Ikejima, K., Honda, H., Kitamura, T., Takei, Y., Sato, N., 2000. Glycine prevents apoptosis of rat sinusoidal endothelial cells caused by deprivation of vascular endothelial growth factor. Hepatology 32 (3), 542–546. https://doi.org/10.1053/jhep.2000.16605.

Zhao, Y., Li, Y., Wang, J., Manthari, R.K., Wang, J., 2018. Fluoride induces apoptosis and autophagy through the IL-17 signaling pathway in mice hepatocytes. Arch. Toxicol. 92 (11), 3277–3289. https://doi.org/10.1007/s00204-018-2305-x.

Zhong, Z., Jones, S., Thurman, R.G., 1996. Glycine minimizes reperfusion injury in a low-flow, reflow liver perfusion model in the rat. Am. J. Physiol. 270 (2 Pt 1), G332–G338. https://doi.org/10.1152/ajpgi.1996.270.2.G332.

Zhou, B.H., Zhao, J., Liu, J., Zhang, J.L., Li, J., Wang, H.W., 2015. Fluoride-induced oxidative stress is involved in the morphological damage and dysfunction of liver in female mice. Chemosphere 139, 504–511. https://doi.org/10.1016/j.chemosphere.2015.08.030.